Geomorphology 219 (2014) 192–199

Contents lists available at ScienceDirect

Geomorphology

journal homepage: www.elsevier.com/locate/geomorph

Boulder weathering in McMurdo Dry Valleys, Antarctica

Jaakko Putkonen [a,*], Daniel Morgan [b], Greg Balco [c]

[a] Harold Hamm School of Geology and Geological Engineering, MS 8358, University of North Dakota, Grand Forks, ND 58202, USA
[b] Department of Earth and Environmental Sciences, Vanderbilt University, Nashville, TN, USA
[c] Berkeley Geochronology Center, Berkeley, CA, USA

ARTICLE INFO

Article history:
Received 2 April 2013
Received in revised form 2 May 2014
Accepted 14 May 2014
Available online 22 May 2014

Keywords:
Boulder weathering
Erosion
Regolith
Antarctica
McMurdo Dry Valleys

ABSTRACT

Earth's dynamic surface undergoes a continuous cycle of mountain building and denudation. One of the important links in this cycle is the break-up and comminution of the rocks that allows for effective transportation of debris by surface processes. The starting and end points in this transformation are well known: bedrock and boulders on one end and silt and clay on the other. However, the existing knowledge of the rates and processes responsible of the intermediate steps is currently limited. To fill this gap in knowledge we studied boulders and their weathering products in the McMurdo Dry Valleys, Antarctica, that have been weathering for hundreds of thousands of years sub-aerially exposed at the ground surface. Our study boulders of locally distinct lithology have trails of rock fragments leading downhill revealing the rate of weathering and subsequent transport rate of the fragments. The rock fragments emanate from the source boulder and decrease in size as the distance downslope increases. We measured the fragment sizes and distances for various lithologies on varying slope angles. We found that large fragments up to 0.4 m in diameter can be transported up to 60 m downslope by unknown processes. The total length of the fragment trail increases with the slope angle. The maximum transport distances of sandstone boulders are approximately 10 times longer than other lithologies, which may be explained by the larger observed fragment sizes of the sandstones. On the other hand measurements of the smaller, generally less than 0.04 m diameter fragments that are transported by wind, revealed much shorter transport distances (<10 m). To gain insights of the boulder and resulting fragment weathering rates we constructed a boulder weathering-fragment transport computer model. The model is based on simple rules and probabilities that describe the weathering and transportation. The model is constrained by the observed fragment size distribution, fragment distribution in space, fragment size/distance relationship, and other observed properties of the fragments. This model allows us to determine the weathering rates of the source boulder and the resulting fragments on the ground, and the fragment size dependent transport rate that are consistent with the observations. Our modeling suggests that the boulders on average spall a fragment over 250 times more often than the resulting fragments re-break and that the currently observed fragment transport rate is consistent with our modeled long term average transport rate.

1. Introduction

As generally recognized by geologists, boulder comminution is a necessary part of the rock cycle. The rocks and boulders need to disintegrate for effective transport to take place. Especially in the arid areas where fluvial and glacial transport events are rare the comminution is a prerequisite for transporting the surficial mineral matter by eolian processes.

The processes that are responsible of the physical weathering have been studied for over a century and several theories have been set forth (e.g. Washburn, 1979, pp. 73–79). The effects of hydrofracturing and explosive frost shattering are found to be important in the Arctic where water is abundant (e.g. Mackay, 1999). In arid areas thermal stresses induced by uneven temperature distribution in the rock can lead to either deep cracking (McFadden et al., 2005) or granular disintegration or spalling of a thin surficial layer (Hall, 1999; Hall and Andre, 2003; Hall et al., 2008; McKay et al., 2009; Eppes and Griffing, 2010).

Much disagreement still exists on the primary physical weathering process in arid environments and its effectiveness. It is suggested that the weathering rate is clast size dependent as a finite thickness is required to develop a thermal gradient inside the clast. The smallest clasts would be isothermal due to relatively high thermal diffusivity of rock. Only larger clasts would develop large enough thermal gradients due to external temperature variations, driven by radiation, clouds, rain, and wind (McFadden et al., 2005). Therefore the expectation is that in an environment where thermally induced cracking is the primary weathering agent the rate of fragmentation is significantly slower

* Corresponding author. Tel.: +1 701 777 3213.
E-mail address: jaakko.putkonen@und.edu (J. Putkonen).

http://dx.doi.org/10.1016/j.geomorph.2014.05.012
0169-555X/

for small clasts (diameter ~ <0.1 m) than it is for boulders (diameter ~ 0.5 m).

Long term, size-dependent rock sorting has been recognized in arid and semi-arid environments and has been attributed to both transport and further comminution of the fragments (e.g. Melton, 1965; McGrath et al., 2013). However, no direct observations of long term (~100's kyrs) weathering of individual boulders and fragments exist. We present field observations aided by simple computer modeling of boulder and clast weathering rates over 600 kyrs from a hyperarid cold desert, the McMurdo Dry Valleys, Antarctica. The field site offers unique opportunities for studying surface processes due to the slow rate of sediment transport and degradation of the landscape (Putkonen et al., 2008a,b; Morgan et al., 2010a,b).

In our research we are not concerned with the particular weathering process (including hydrofracturing, thermally induced fragmentation, salt weathering, etc.), instead we observe and model the source boulder break-up rate and compare that with the fragment weathering rate, and related transport over their lifespan. By using the simplest possible model assumptions, and independent dating data, we reproduce the fragment size and spatial patterns and draw conclusions of the processes and rates.

In this paper we aim to describe our observations of the fragment size and spatial distribution patterns in the field, and analyses of these data with the help of a computer model that obeys simple probabilistic rules and clast size patterns. And finally we ask what these patterns can tell us collectively of the boulder weathering, clast transportation, and clast re-breaking in a cold desert environment.

2. Methods

All the boulders we studied are on sloping surfaces. As the source boulders, which were all approximately a meter in diameter with a few exceptions, weather on a slope, the resulting rock fragments fall on the base of the boulder. Over time the fragments are being transported downhill from the source boulder. This results in a trail of rock fragments on the downhill side of the source rock that is sometimes visible from hundreds of meters away. We call such a fragment pattern a fragment trail (Fig. 1).

In order to determine how far the individual fragments have been transported from the source boulder, we chose boulders that were of distinct lithology compared to the majority of the boulders and pebbles in a given location and slope. For example on a slope that was littered with dolerites we chose a sandstone source rock which was distinct in color and the weathered fragments could be effectively located.

Fragment trails can be found in other parts of the Earth as well. For example in the eastern Sierra Nevada (USA) we have observed short and sparse fragment trails. It appears that in more humid and geologically active environments the weathered fragments are relatively quickly transported away, further re-broken, or otherwise are not nearly as conspicuous as they are in the field area in Antarctica.

In our field area in the McMurdo Dry Valleys we encountered two types of fragment trails: 1) long trails that are 10–60 m long and include fragments that are up to 0.4 m in diameter, and 2) short trails that are <10 m long and typically contain fragments that are <0.04 m in diameter. Three different approaches were used to characterize the fragments and their relative locations in the field. All of these methods account only for exposed fragments on the surface, however, this area is known to degrade over long periods of time (Putkonen et al., 2008a) and thus the burial of the fragments is unlikely.

Method 1 for detailed analyses of the short trail fragments we measured the intermediate dimension of each fragment, coming from the source boulder, that was found in the fragment trail. Simultaneously, the 2-dimensional location of the fragment was recorded in the coordinate system consisting of 20 cm by 20 cm squares. This allowed us to determine the size and the location of each individual fragment that originated from the given source boulder.

Method 2 detailed analyses with a tape measure. The tape measure was laid down downslope from the source boulder along the highest concentration of the fragments. The location and intermediate dimension of every fragment touching the tape were logged. Then a second tape was laid perpendicular to the initial direction at the base of the source boulder and every full meter thereafter downhill from the source boulder. This created a baseline and spokes pattern that allowed for economic characterization of the fragment plume.

Method 3 analyses of the trails were done with a tape measure that was laid down straight along the highest concentration downhill from the source boulder. We then proceeded to record the distance and intermediate axis of every fragment that touched the tape measure. This method allowed us to collect data on large number of source boulders but only allowed for estimation of the total fragment population. However, we used these data to determine the maximum transport distances on a given slope angle and source boulder lithology. For these purposes the technique is adequate.

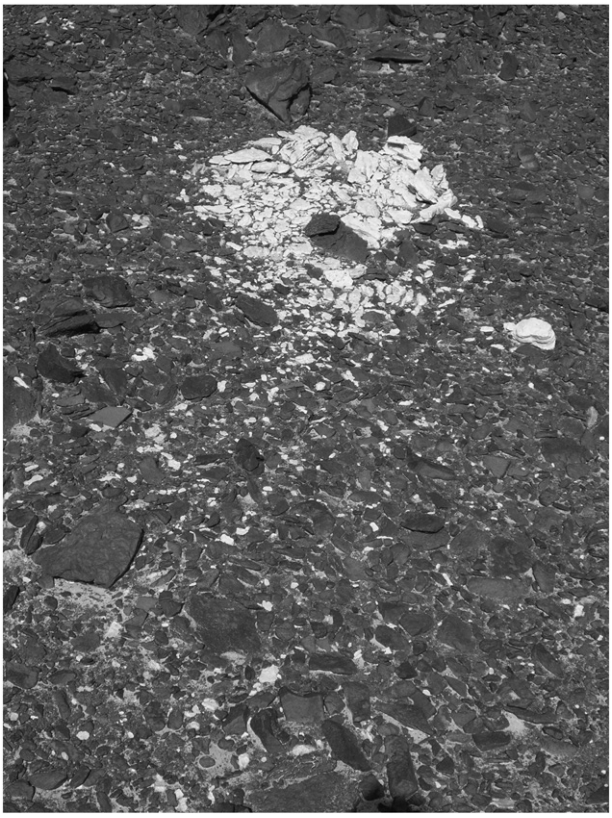

Fig. 1. Short fragment trail formed of fragments that broke off the sandstone source boulder. After breaking off the fragments have been transported downhill on the ground.

In two field seasons (2004–2005, and 2005–2006) we measured eight short trails and over fifty long trails in the McMurdo Dry Valleys. The data consist of paired location and size data for all recorded rock fragments. We also determined the lithology, location and the dimensions of the source rock (Table 1).

With methods 1 and 3 the fragment travel distances were measured to the nearest 5 mm, with method 2 within 20 cm brackets. The fragment dimensions were measured with 1 mm accuracy. We measured only fragments whose intermediate dimensions were equal or larger than 5 mm.

Table 1
Source rock identification number, general location and coordinates, dimensions (cm) and lithology of the analyzed boulders.

Id	Coordinates	Size (cm)	Lithology
Arena and Beacon Valley			
1	S 77 51.417′, E 160 57.765′	40 × 25 × 4	Granite
2	S 77 51.323′, E 160 58.072′	10 × 16 × 3	Granite
3	S 77 51.315′, E 160 58.113′	4 × 26 × 0	Granite
9	S 77 50.424′ E 160 56.877′	20 × 30 × 10	Granite
10	S 77 50.414′ E 160 56.911′	200 × 300 × 100	Granite
11	S 77 49.642′ E 160 41.230′	N/A	Granite
4	S 77 51.525′, E 160 57.874′	60 × 80 × 32	Sandstone
5	S 77 51.526′, E 160 57.867′	80 × 70 × 30	Sandstone
6	S 77 51.578′, E 160 57.822′	70 × 90 × 40	Sandstone
7	S 77 51.452′, E 160 57.657′	40 × 60 × 15	Sandstone
8	S 77 50.458′, E 160 56.788′	80 × 60 × 50	Sandstone
13	S 77 49.424′ E 160 41.589′	N/A	Sandstone
Hart and Meserve Glaciers			
24	S 77 30 587′ E 162 22.431′	15 × 10 × 8	Granite
32	S 77 30.532′ E 162 20.388′	37 × 38 × 3	Granite
34	S 77 30.504′ E 162 20.476′	52 × 27 × 20	Granite
35	S 77 31.347′ E 162 17.133′	40 × 20 × 4	Granite
37	N/A		Granite
38	S 77 31.328′ E 162 16.913′	24 × 15 × 2	Granite
39	S 77 31.312′ E 162 16.919′	40 × 25 × 2	Granite
41	S 77 31.295′ E 162 16.970′	17 × 42 × 1	Granite
48	S 77 31.066′ E 162 18.769′	40 × 30 × 3	Granite
50	S 77 31.047′ E 162 18.785′	30 × 55 × 2	Granite
51	S 77 31.043′ E 172.18.808′	60 × 35 × 25	Granite
52	S 77 31.031′ E 162 18.833′	70 × 75 × 2	Granite
55	S 77 31.024′ E 162 18.610′	16 × 30 × 12	Granite
56	S 77 31.007′ E 162 18.632′	35 × 30 × 3	Granite
59	S 77 30.979′ E 162 18.694′	50 × 60 × 3	Granite
60	S 77 30.977′ E 162 18.687′	100 × 110 × 20	Granite
61	S 77 30.872′ E 162 18.250′	140 × 80 × 10	Granite
64	S 77 30.747′ E 162 18.652′	110 × 170 × 10	Granite
65	S 77 30.752′ E 162 18.615′	90 × 60 × 7	Granite
66	S 77 30.794′ E 162 18.313′	80 × 90 × 25	Granite
67	S 77 30.701′ E 162 17.875′	20 × 38 × 2	Granite
69	S 77 30.681′ E 162 17.842′	50 × 35 × 5	Granite
70	S 77 30.671′ E 162 17.886′	85 × 80 × 10	Granite
29	S 77 30.530′ E 162 22.325′	50 × 20 × 1.5	Granite
19	S 77 30.588′ E 162 22.394′	130 × 110 × 15	Metamorphic
20	S 77 30.531′ E 162 22.355′	35 × 20 × 15	Metamorphic
21	S 77 30.506′ E 162 22.263′	50 × 65 × 15	Metamorphic
22	S 77 30.503′ E 162 22.244′	35 × 40 × 5	Metamorphic
23	S 77 30.543′ E 162 22.325′	20 × 30 × 3	Metamorphic
27	S 77 30.552′ E 162 22.319′	60 × 100 × 15	Metamorphic
28	S 77 30.537′ E 162 22.298′	25 × 20 × 2	Metamorphic
30	S 77 30.526′ E 162 22.309′	130 × 120 × 2–8	Metamorphic
31	S 77 30 547′ E 162 20.322′	20 × 15 × 2	Metamorphic
36	S 77 31.360′ E 162 17.073′	48 × 52 × 6	Metamorphic
40	S 77 31.292′ E 162 16.978′	35 × 55 × 2	Metamorphic
42	S 77 31.300′ E 162 17.018′	47 × 32 × 4	Metamorphic
43	S 77 31.308′ E 162 17.064′	90 × 70 × 35	Metamorphic
44	S 77 31.216′ E 162 17.365′	37 × 22 × 0	Metamorphic
46	S 77 31 070′ E 162 18.740′	30 × 28 × 4	Metamorphic
47	S 77 31.071′ E 162 18.746′	60 × 40 × 7	Metamorphic
48	S 77 31.066′ E 162 18.769′	40 × 30 × 3	Metamorphic
49	S 77 31.046′ E 162 18.753′	37 × 10 × 15	Metamorphic
58	S 77 30.980′ E 162 18.689′	58 × 50 × 5	Metamorphic
62	S 77 30.850′ E 162 18.464′	42 × 54 × 5	Metamorphic
63	S 77 30.825′ E 162 18.577′	60 × 70 × 10	Metamorphic
68	S 77 30.680′ E 162 17.842′	50 × 40 × 1	Metamorphic
71	S 77 30.674′ E 162 17.866′	40 × 30 × 3	Metamorphic
72	S 77 30.674′ E 162 17.866′	25 × 18 × 2	Metamorphic
73	S 77 30.675′ E 162 17.843′	35 × 30 × 4	Metamorphic
74	S 77 30.678′ E 162 17.827′	33 × 26 × 3	Metamorphic
75	S 77 30.673′ E 162 17.805′	22 × 15 × 2	Metamorphic
Koenig valley			
14	S 77 36.758′ E 160 47.139′	100 × 200 × 100	Sandstone
15	S 77 36.635′ E 160 44.920′	450 × 230 × 300	Sandstone
16	S 77 36.555′ E 160 45.051′	500 × 400 × 250	Sandstone
17	S 77 36.963′ E 160 46.989′	N/A	Sandstone
18	S 77 30.716′ E 162 17.637′	200 × 170 × 140	Sandstone

Table 1 (*continued*)

Id	Coordinates	Size (cm)	Lithology
Other areas			
25	S 77 30.579′ E 162 22.384′	15 × 8 × 2	Sandstone
26	S 77 30.567′ E 162 22.326′	25 × 45 × 7	Sandstone
53	S 77 31.028′ E 162 18.774′	22 × 35 × 3	Sandstone
54	S 77 31.024′ E 162 18.609′	12 × 14 × 2	Sandstone

2.1. Field area

McMurdo Dry Valleys is located approximately 100 km West of McMurdo station, the largest permanent residence in Antarctica. The Dry Valleys have a cold desert climate that receives less than 100 mm precipitation in the form of snow a year. The mean annual air temperature varies with altitude and ranges from about −21 °C (Fountain et al., 1999) to −24 °C in the higher elevations (Putkonen et al., 2003). Running melt water is typically observed at lower altitudes and occasionally witnessed in the alpine valleys above 1000 masl.

Based on glacial geology, ash chronology, and cosmogenic isotopes the field area has been ice free for millions of years (Denton et al., 1993; Marchant et al., 1993a,b, 1996; Marchant and Denton, 1996; Putkonen et al., 2008a; Morgan et al., 2010a,b). The ice free hyper arid cold desert has some of the slowest recorded surface transport rates on Earth (Putkonen et al., 2008b) which enabled us to observe the rock fragments that have been in transport for hundreds of thousands of years. On par with the slow surface transport is the generally slow regolith degradation of about 1 m/Myr (Putkonen et al., 2008a; Morgan et al., 2010a,b) and longevity of surficial boulders (Brown et al., 1991; Brook et al., 1993, 1995; Schäfer et al., 1999, 2000; Staiger et al., 2006; Nicola et al., 2009).

The boulders that we observed in the field area (Table 1) were identified as granite, metamorphic, dolerite, or sandstone. Granitic rocks crop out in the lowest elevations of the Wright Valley, however, the majority of our observations come from higher elevation alpine valleys and therefore we suspect that our study boulders originate from outside of the currently ice free McMurdo Dry Valleys area as noted for example by Sugden et al. (1995). Abundant sandstone and dolerite are found locally in Devonian Beacon Supergroup, as well as a lesser volume of Precambrian metamorphic rocks of the Koettlitz group (Gunn and Warren, 1962).

2.2. Model

To gain insights into the boulder weathering, fragment transport and subsequent further breakup of the fragments we constructed a simple probabilistic computer model that allows for rigorous evaluation of relationships and effects of various parameters and drivers on the resulting fragment size and spatial patterns.

The guiding principles for this computer model are to keep it as simple as possible, make the fewest and simplest possible assumptions, incorporate no physics, and have it constrained by observations. The model operation and the parameters are described in the following paragraphs.

Boulder break rate is a prescribed probability that describes how often the source boulder breaks and produces a fragment. At every time step of the model (100 yrs) the prescribed boulder break rate probability (a number between 0 and 1) is checked against a randomly generated number in the model (between 0 and 1) which then is used to determine whether or not a fragment is generated at this time. The probability is constrained by the fit between the model generated and the observed fragment spatial and dimensional distributions.

Fragment break rate is a prescribed probability (between 0 and 1) that describes how often the rock fragment re-breaks while in transport on the ground. At every time step each existing fragment is addressed and a randomly generated number in the model (between 0 and 1) is checked against the prescribed fragment break probability to determine whether or not that particular fragment is re-broken at this time step. The probability is constrained by the fit between the model generated and the observed fragment spatial and dimensional distributions.

Fragment transport rate describes how fast the fragments are being transported on the ground. The fragments are being transported downhill based on their size and the local slope angle:

$$L = \left(D_{max} - D_{fragment}\right) * (dy/dx) * M * dt \quad (1)$$

where L (m) is the distance the fragment of a given size is transported a given time step, D_{max} is the max size of a fragment that is transported (0.1 m), $D_{fragment}$ is the intermediate diameter of the fragment in question (m), dy (m) is a vertical distance the surface is raised over a horizontal distance dx (m) and therefore dy/dx describes the slope gradient, M is the transport parameter (yr^{-1}), and dt is the length of the model time step (yrs).

It has been previously established that the regolith transport in Dry Valleys is by eolian processes and no depth distributed creep has taken place for millions of years (Putkonen et al., 2008a). It is well known that eolian processes move the particles based on their size. Moreover smaller particles move more readily and more often than larger particles (Bagnold, 1941). However, we have observed fragment movement in the field that involves just a few pebbles per square meter per year (Putkonen et al., 2008b) therefore it is unclear what would be the most appropriate relationship between the wind speed and the fragment transport and how this would translate into total transport per given time period. For these reasons we used a simple linear relationship between fragment size and transport rate. The fragment transport is assumed to be zero for fragments with intermediate diameter ≥100 mm and highest (the value reported in Table 1) for fragments whose intermediate diameter is 5 mm which is the smallest tracked diameter in the model. At every time step in the model all the fragments are transported based on their size and the slope angle. Although the model treats the fragment transport as a constant and continuous process, it can be viewed as a model representation of a long term average transport of intermittent, and on short time span, chaotic movement of surficial fragments.

Maximum model time describes what is the time span that the source boulder has been shedding fragments. It has been shown that Dry Valleys have remained ice free for millions of years (Putkonen et al., 2008b; Morgan et al., 2010a,b). Therefore the surface deposits generally originate from the last ice excursions into the valleys that took place millions of years ago and that have been dated by Ar/Ar on related ash deposits (Marchant et al., 1993a,b, 1996) and the accumulation of the cosmogenic isotopes in the bulk samples of the drift itself (Morgan et al., 2010a,b).

Although surficial boulders in the mid and northern latitudes degrade relatively rapidly, it is not uncommon to find boulders of great antiquity in the Antarctica. Some of the boulders that are found on the drifts in Dry Valleys have been independently dated by the in situ accumulation of cosmogenic nuclides. All researchers dating boulders in the Dry Valleys have found boulders whose exposure ages are in millions of years although younger boulders have been found on the youngest drifts (Brook et al., 1995; Ivy-Ochs et al., 1995; Schäfer

et al., 1999, 2000; Margerison et al., 2005; Staiger et al., 2006; Swanger et al., 2011). Although boulders are known to survive for millions of years it is also conceivable that individual boulders and deposits may originate from local rockfalls, landslides, or unstable boulders eventually rolling down the hillslopes. Therefore an exposure age of a given boulder is not obvious. The exposure histories of the particular boulders that we measured have not been determined. However, it has been determined by cosmogenic nuclides in bulk sediments that the surficial pebbles (1–2 cm thickness of the regolith at the ground surface) carry a distinctly different exposure signature from the ancient glacial drifts (Morgan et al., 2010a,b). Therefore we assign an exposure age of 600 kyrs to our modeled boulders/fragments based on actual measured exposure ages of surficial pebbles in the same field area (Morgan et al., 2010a,b).

Slope in the model is the local measured slope angle. The actual slope angles were measured next to the modeled boulders and are used in the model.

Initial fragment size distribution describes the size distribution of fragments that break off from the source boulder. Our observations of fragments found next to the source boulders suggest that smaller grain sizes are more abundant than larger grain sizes. However, large variation exists between populations. To avoid biasing the model with a too finely tailored grain size distribution we used an exponential grain size distribution. The initial fragment size distribution is described by the following function:

$$y = x^2 - 2x + 1 \quad (2)$$

where y is between 0 and 1 and x is between 0 and 1. In the model a randomly generated number (between 0 and 1) is entered for x in the above function. This yields the length of the intermediate axis when the resulting y is multiplied with pertinent maximum fragment size. This scheme produces fragments randomly between 5 mm and the maximum assigned fragment size. However, due to the functional dependency that is given above the smaller grain sizes are statistically more prevalent than larger grain sizes.

The following paragraphs describe conceptually the structure and operation of the computer model. The model consists of an execution loop that represents the progression of time. During every time step various functions are applied. These functions generate fragments from the source boulder, move the fragments forward on the ground, and re-break the fragments based on simple rules. These rules, as described above, are designed to reproduce the essential patterns that are observed in the field and in particular reveal the rates of weathering and surface transport. This model is not based on rock physics or observations of rock physical properties. However, this model attempts to capture the rates of primary processes by looking at the resulting fragment patterns regardless of what those processes are. By doing this we hope to gain insights of the weathering and surface transport in the cold desert of which little is known currently.

The computer model progresses through following segments (A and B explained below) at 100 model year time steps. This means that for the 600 kyrs modeled surface the model will run through following sections 6000 times.

A) For the starter the model generates a random number (between 0 and 1) which is compared to the source boulder break probability (between 0 and 1). If the random number is smaller than the break probability a fragment is generated. To determine the length of the intermediate axis of the freshly broken fragment a second random number is generated by the model. Based on the original fragment size distribution (described in prior paragraphs) this random number is entered into the function that returns the corresponding fragment size (between 0 and 1). This in turn yields the length of the intermediate axis when multiplied by the maximum allowed fragment size. The distance of the fresh fragment from the source boulder is set to zero. In other words the fragment falls at the base of the source boulder. At a given time step a maximum of one fresh fragment may be produced.
B) Within the same time step the program then proceeds to process all the existing fragments that are lying on the ground (generated during prior time steps). Every existing fragment is visited one at a time. As an example the procedure is here described in detail for one pre-existing fragment. First the fragment is moved downhill based on the prescribed transport coefficient and the local slope angle. After the downhill transport a fresh random number (between 0 and 1) is generated. This random number is evaluated against the fragment re-break probability. If the random number is smaller than the re-break probability the fragment is re-broken. The existing fragment is randomly broken into two fragments whose combined intermediate axis length equals the original single fragment intermediate axis length. The two new fragments are assigned the same distance from the source boulder as the single fragment had prior to re-breaking. If at any time a fragment intermediate axis becomes smaller than 5 mm it is removed from the database and no longer tracked by the model (5 mm is the smallest fragment size observed in the field).

This concludes one model loop which is also one time step. At this point the model execution returns to the beginning (section A above), the model time is advanced by one time step (100 yrs) and the sequence of above sections is rerun. This loop is redone until the model time reaches the prescribed surface age at which point the resulting fragment statistics are compared to the observed fragment statistics.

2.2.1. Best fit model parameters

To find the combination of model parameters for each of the eight short trails that produced the best fit between the observed and modeled boulder fragments we determined the least squared differences between: 1) modeled and observed average fragment sizes versus transport distance, 2) modeled and observed fragment size distributions, and 3) modeled and observed fragment counts versus distance from source. In order to construct a single least squared value each of the three least square differences was normalized to its respective maximum value and the resulting three values were averaged. Due to different units of all three least squares the resulting number has no concrete meaning and is considered dimensionless. However, a smaller number reflects a better overall fit and this guided our determination of the below listed parameters (Table 2).

The model parameters that were varied to optimize the fit between observations and corresponding model results are: boulder break rate (how fast the source boulder breaks down), fragment re-break rate (how often the fragments laying on the ground re-break), maximum fragment diameter (the length of the intermediate axis of the largest

Table 2
The parameters that yielded the best fit between the observations and model. Parameter statistics for all eight short trails.

	Mean	St. dev	Median	Min	Max
Transport parameter (yr^{-1})	$1.91 * 10^{-4}$	$1.95 * 10^{-4}$	$7.97 * 10^{-5}$	$4.12 * 10^{-5}$	$5.71 * 10^{-4}$
Boulder break probability (%)	$5.33 * 10^{-2}$	$4.95 * 10^{-2}$	$4.01 * 10^{-2}$	$1.75 * 10^{-2}$	$1.70 * 10^{-1}$
Fragment re-break probability (%)	$1.95 * 10^{-4}$	$1.84 * 10^{-4}$	$1.31 * 10^{-4}$	$7.80 * 10^{-5}$	$6.44 * 10^{-4}$

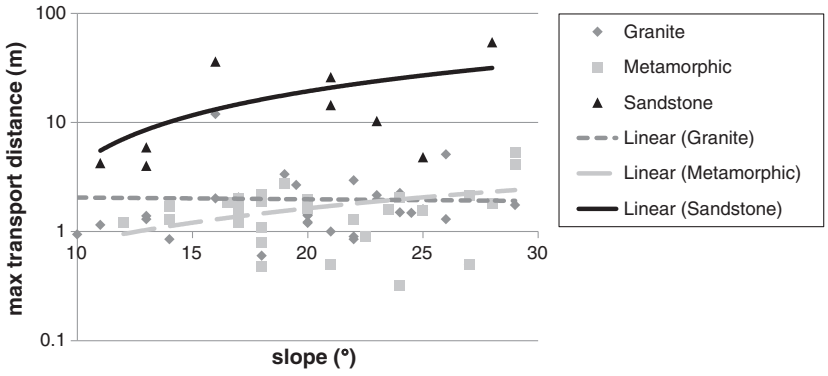

Fig. 2. All measured fragment trail lengths (>10 m) for three distinct lithologies. The sandstone fragment trails are generally much longer than metamorphic or granitic trails. The trail lengths correlate weakly with the local slope. The trend line for granite trails is level due to the one outlier at 16° slope and 11.9 m maximum travel distance. The linear trend lines appear curved in this semi-log space.

possible fragment), and fragment transport coefficient (coefficient that describes the average annual rate of movement of a fragment on the ground when combined with the fragment size and the local slope angle).

3. Results

We run the parameter optimizing scheme separately for all eight short fragment trail boulders that were measured in the field. These runs yielded the best fit combinations of the above listed parameters.

3.1. Long trails

We measured a total of over 70 long trails that include trails up to 60 m long and include fragments that are up to 0.4 m in diameter. A linear trend through the trail lengths versus slope angles suggests that the lengths increase with increasing slope angle within a given lithology (Fig. 2). Moreover, the longest of the maximum trail lengths for sandstone fragments were approximately ten times longer than metamorphic or granitic trails.

The fragment size distributions for metamorphic and granitic rocks were nearly identical. However, the sandstone fragments were on average about twice the size of metamorphic or granitic fragments (Fig. 3).

3.2. Short trails

We made detailed measurements of a total of eight short trails that are <10 m long and the fragments are mostly <40 mm in diameter. The measured boulders include four sandstones, two metamorphic, one dolerite, and one granitic source boulder. The small fragments related to the short trails are intermittently transported by wind (Lancaster, 2002; Putkonen et al., 2008b; Gillies et al., 2012). Our modeling of the fragment size and spatial distributions suggests that the mean fragment transport rate is $1.9 * 10^{-4}$ yr^{-1} (Table 2). The resulting fragment size distributions and transport patterns closely mimic the observations (Fig. 4).

Boulder break rate determines the frequency that the new fragments are broken off the source boulder. The modeling suggests that the boulders break at an annual break-up probability of $5.3 * 10^{-2}$%. Mean annual fragment re-break probability is $1.9 * 10^{-4}$%.

The local slope angles for the short trails ranged from 10.5° to 27.0°. The maximum transport distances do not correlate with slope angles for the eight short trails.

4. Discussion

In addition to the detailed observations on short trails (<10 m) we also measured long trails in the field, but assume that the processes responsible of the much larger fragment sizes and longer transport distances than found with the short trails must include more effective means of transport than just wind. We don't attempt to explain how or when the fragments were transported and generally concentrate on the short trails and the smaller fragments found there.

The model results suggest that the boulder break rate is over 250 times faster than the fragment re-break rate. This finding can be logically confirmed. If fragments were re-breaking at a same rate as the source boulder, there would be no fragments anywhere to be found. They

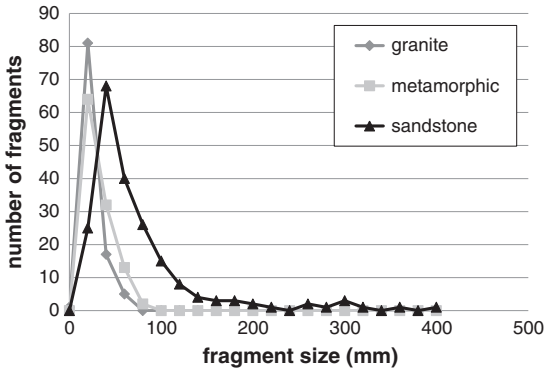

Fig. 3. Observed grain size distributions for three lithologies. The analysis is based on five centerline measurements per lithology comprising of a total of 419 fragments. The metamorphic and granite fragment distributions are identical, however, the sandstone fragments are generally larger.

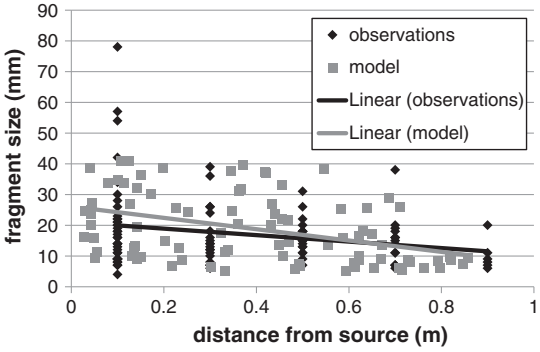

Fig. 4. One realization of the probabilistic weathering and fragment transport model output (BT2). The diamonds are observations that are grouped together by the measurement coordinates. The squares represent the modeled fragments. Similarities between the linear trends of the observed and modeled fragments suggest that the model captures statistically the weathering and the transport of the fragments.

would quickly disintegrate and turn into sand. This would be dictated by the fact that the fragment destruction would be faster than the production of new fragments. Therefore the fact that the fragments are abundant in this field area proves that the fragment break-up rate is slower than the initial source boulder break-up rate.

The boulder and fragment break rates are dependent on the modeled boulder age. Although we find the 600 kyrs to be the best estimate based on direct measurements of surficial pebbles in the same field area it is possible that the boulders are significantly older as boulder ages and glacial drifts in the area generally show. The older than modeled boulder and pebble ages would make our boulder and pebble break rates the minimum estimates, but importantly, would not affect the relative rate of boulder break rate being over 250 times faster than the fragment re-break rate.

As the model used in this study is descriptive and does not incorporate any physics it is prudent to consider if these results are non-unique. First, to assess if the observed grain size distribution in the field is inherited from the original breaking of the source boulder and not altered after deposition on the ground. We analyzed the grain size distribution of fragments next to the boulder and fragments at the far downslope end of the transported plume. It was clear that the largest grains are lost and the distribution is skewed towards smaller grain sizes. Therefore, we suggest that the fragments are further broken on the ground.

Second, our modeled boulder weathering rate (fragment break off rate of the source boulder) applied to a typical boulder of 0.5 m intermediate diameter would lead to a total disintegration of the source boulder in few tens of millions of years. Although such a time span is excessive when compared to boulders in more temperate and humid regions this boulder lifespan is consistent with boulder ages in millions of years that have been obtained in this field area (Brown et al., 1991; Brook et al., 1993, 1995; Schäfer et al., 1999, 2000; Staiger et al., 2006; Nicola et al., 2009).

Third, as the fragment size, count, and spatial distributions are controlled by fragment production rate (source boulder break-up rate) and the fragment destruction rate (fragment re-break rate) is it possible to maintain the same fragment count and transport distance with much higher rates of both fragment production and destruction? It turns out that either much higher rates or much lower rates of fragment production and destruction produce a much worse fit between observations and modeled patterns. High rates lead to either too many fragments or too short transport distances. Low rates lead to lack of fragments.

The long term fragment transport rates reported here are orders of magnitude smaller than the modern particle creep values determined in the Wright Valley (McMurdo Dry Valleys) gravel dune field (Gillies et al., 2012). However, the long term transport rates are similar to the modern transport rates determined in the same field locations where the fragment trails were studied (Putkonen et al., 2008b). This difference may be simply explained by the short observation periods of both abovementioned studies and year to year variations in the eolian transport at a given field location.

5. Conclusions

Our observations and computer modeling of the boulder and fragment weathering and fragment transportation showed that fragment transport in the McMurdo Dry Valleys, Antarctica is dependent on the slope. On average the fragments have traveled farther on steeper slopes than on gentle slopes although large variability exists between individual fragment trails. Those observations also showed that the sandstone fragments had traveled almost 10 times the distance that the metamorphic and granitic fragments had traveled. This may be partially explained by the fact that the sandstone fragments were found to be on average about twice the size of the metamorphic or granitic fragments.

The computer modeling of short fragment plumes (<10 m) where our most detailed data comes from suggests that the source boulders break and produce a rock fragment over 250 times more often than the resulting fragment re-breaks. This finding is supported by the fact that if the source boulders were breaking at a same rate as the resulting fragments there would be no fragments anywhere to be found as the fragments would disintegrate into sand faster than being replenished by breaking of the source boulder. Based on our modeling the source boulder breaks and produces a fresh fragment on average once in every 1.9 kyrs, whereas the existing fragments re-break on average only once in 510 kyrs.

These results are consistent with the thermally induced boulder break-up model (e.g. McFadden et al., 2005; Warren et al., 2013). When a sufficiently large boulder (~0.5 m in diameter) is forced by diurnal or weather related changes in the ambient temperature and surface heating it develops domains that are in greatly different temperatures. This leads into internal strains and stresses that can fracture the boulder. The concurrent differences in the internal temperatures are explained by sufficient size of the boulder and relatively small thermal diffusivities as shown by thermal modeling and field observations (Warren et al., 2013). On the other hand a small fragment (smaller than about 0.1 m in diameter) has small volume and is therefore almost isothermal even when ambient thermal forcing is changing and therefore the fragment is much less likely to re-break due to thermally induced stresses.

Acknowledgments

We were greatly helped in the Dry Valleys by field team members: K. Craig, J. Connolly, N. Turpen, and B. O'Donnell. We are grateful for logistical support by Raytheon. This research was funded by the NSF grant number ANT-0838968.

References

Bagnold, R.A., 1941. The Physics of Blown Sand and Desert Dunes. Methuen, London, (265 pp.).
Brook, E.J., Kurz, M.D., Ackert, J.R.P., Denton, G.H., Brown, E.T., Raisbeck, G.M., Yiou, F., 1993. Chronology of Taylor Glacier advances in Arena Valley, Antarctica, using in situ cosmogenic ^{3}He and ^{10}Be. Quat. Res. 39, 11–23.
Brook, E.J., Brown, E.T., Kurz, M.D., Ackert, R.P., Raisbeck, G.M., Yiou, F., 1995. Constraints on age, erosion, and uplift of Neogene glacial deposits in the Transantarctic Mountains determined from in situ cosmogenic ^{10}Be and ^{26}Al. Geology 23, 1063–1066.
Brown, E.T., Edmond, J.M., Raisbeck, G.M., Yiou, F., Kurz, M.D., Brook, E.J., 1991. Examination of surface exposure ages of Antarctic moraines using in situ produced ^{10}Be and ^{26}Al. Geochim. Cosmochim. Acta 55, 2269–2283.
Denton, G.H., Sugden, D.E., Marchant, D.R., Hall, B.L., Wilch, T.I., 1993. East Antarctic ice sheet sensitivity to Pliocene climatic change from a Dry Valleys perspective. Geogr. Ann. 75A, 155–204.
Eppes, M.C., Griffing, D., 2010. Granular disintegration of marble in nature: a thermal–mechanical origin for a grus and corestone landscape. Geomorphology 117, 170–180.
Fountain, A.G., Lewis, K.J., Doran, P.T., 1999. Spatial climatic variation and its control on glacier equilibrium line altitude in Taylor Valley, Antarctica. Glob. Planet. Change 22, 1–10.
Gillies, J.A., Nickling, W.G., Tilson, M., Furtak-Cole, E., 2012. Wind-formed gravel bed forms, Wright Valley, Antarctica. J. Geophys. Res. 117 (F04017), 1–19.
Gunn, B.M., Warren, G., 1962. Geology of Victoria Land between the Mawson and Mulock Glaciers. N. Z. Geol. Surv. Bull. 71, 1–157.
Hall, K., 1999. The role of thermal stress fatigue in the breakdown of rock in cold regions. Geomorphology 31, 47–63.
Hall, K., Andre, M.F., 2003. Rock thermal data at the grain scale: applicability to granular disintegration in cold environments. Earth Surf. Process. Landf. 28, 823–836.
Hall, K., Guglielmin, M., Strini, A., 2008. Weathering of granite in Antarctica: II. Thermal stress at the grain scale. Earth Surf. Process. Landf. 33, 475–493.
Ivy-Ochs, S., Schluchter, C., Kubik, P.W., Dittrich-Hannen, B., Beer, J., 1995. Minimum ^{10}Be exposure ages of early Pliocene for the Table Mountain plateau and the Sirius Group at Mount Fleming, Dry Valleys, Antarctica. Geology 23, 1007–1010.
Lancaster, N., 2002. Flux of eolian sediment in the McMurdo Dry Valleys, Antarctica: a preliminary assessment. Arct. Antarct. Alp. Res. 34, 318–323.
Mackay, J.R., 1999. Cold-climate shattering (1974 to 1993) of 200 glacial erratics on the exposed bottom of a recently drained Arctic Lake, Western Arctic Coast, Canada. Permafr. Periglac. Process. 10, 125–136.
Marchant, D.R., Denton, G.H., 1996. Miocene and Pliocene paleoclimate of the Dry Valleys region, southern Victoria Land; a geomorphological approach. Mar. Micropaleontol. 27, 253–271.

Marchant, D.R., Denton, G.H., Sugden, D.E., Swisher, C.C.I., 1993a. Miocene glacial stratigraphy and landscape evolution of the western Asgard Range, Antarctica. Geogr. Ann. 75A, 303–330.
Marchant, D.R., Denton, G.H., Swisher, C.C.I., 1993b. Miocene–Pliocene–Pleistocene glacial history of Arena Valley, Quartermain Mountains, Antarctica. Geogr. Ann. 75A, 269–302.
Marchant, D.R., Denton, G.H., Swisher, C.C.I., Potter, N.J., 1996. Late Cenozoic Antarctic paleoclimate reconstructed from volcanic ashes in the dry valleys region of southern Victoria Land. Geol. Soc. Am. Bull. 108, 181–194.
Margerison, H.R., Phillips, W.M., Stuart, F.M., Sugden, D.E., 2005. Cosmogenic ^{3}He concentrations in ancient flood deposits from the Coombs Hills, northern Dry Valleys, East Antarctica: interpreting exposure ages and erosion rates. Earth Planet. Sci. Lett. 230, 163–175.
McFadden, L.D., Eppes, M.C., Gillespie, A.R., Hallet, B., 2005. Physical weathering in arid landscapes due to diurnal variation in the direction of solar heating. Geol. Soc. Am. Bull. 117, 161–173.
McGrath, G.S., Nie, Z., Dyskin, A., Byrd, T., Jenner, R., Holbeche, G., Hinz, C., 2013. In situ fragmentation and rock particle sorting on arid hills. J. Geophys. Res. 118, 1–12.
McKay, C.P., Molaro, J.L., Marinova, M.M., 2009. High-frequency rock temperature data from hyper-arid desert environments in the Atacama and the Antarctic Dry Valleys and implications for rock weathering. Geomorphology 110, 182–187.
Melton, M.A., 1965. Bris-covered hillslopes of the Southern Arizona desert: consideration of their stability and sediment contribution. J. Geol. 73, 715–729.
Morgan, D., Putkonen, J., Balco, G., Stone, J., 2010a. Quantifying regolith erosion rates with cosmogenic nuclides ^{10}Be and ^{26}Al in the McMurdo Dry Valleys, Antarctica. J. Geophys. Res. 115 (F03037), 1–17.
Morgan, D.J., Putkonen, J., Balco, G., Stone, J.O.H., 2010b. Degradation of glacial deposits quantified with cosmogenic nuclides, Quartermain Mountains, Antarctica. Earth Surf. Process. Landf. 36, 217–228.
Nicola, L.D., Strasky, S., Schlüchter, C., Salvatore, M.C., Akçar, N., Kubik, P.W., Christl, M., Kasper, H.U., Wieler, R., Baroni, C., 2009. Multiple cosmogenic nuclides document complex Pleistocene exposure history of glacial drifts in Terra Nova Bay (northern Victoria Land, Antarctica). Quat. Res. 71, 83–92.
Putkonen, J., Sletten, R.S., Hallet, B., 2003. Atmosphere/ice energy exchange through thin debris cover in Beacon Valley, Antarctica. In: Phillips, M., Springman, S.M., Arenson, L.U. (Eds.), Eighth International Conference on Permafrost, Zurich, Switzerland, July 21–25, 2003. Balkema, Lisse, pp. 913–915.
Putkonen, J., Balco, G., Morgan, D., 2008a. Slow regolith degradation without creep determined by cosmogenic nuclide measurements in Arena Valley, Antarctica. Quat. Res. 69, 242–249.
Putkonen, J., Rosales, M., Turpen, N., Morgan, D., Balco, G., Donaldson, M., 2008b. Regolith transport in the Dry Valleys of Antarctica. In: Cooper, A.K., Barrett, P.J., Stagg, H., Storey, B., Stump, E., Wise, W. (Eds.), Antarctica: A Keystone in Changing World. Proceedings of the 10th International Symposium on Antarctic Earth Sciences. The National Academies Press, Santa Barbara, CA, USA, p. 164. http://dx.doi.org/10.3133/of2007-1047.srp103.
Schäfer, J., Ivy-Ochs, S., Wieler, R., Leya, I., Baur, H., Denton, G.H., Schluechter, C., 1999. Cosmogenic noble gas studies in the oldest landscape on Earth; surface exposure ages of the dry valleys, Antarctica. Earth Planet. Sci. Lett. 167, 215–226.
Schäfer, J.M., Baur, H., Denton, G.H., Ivy-Ochs, S., Marchant, D.R., Schluchter, C., Wieler, R., 2000. The oldest ice on Earth in Beacon Valley, Antarctica: new evidence from surface exposure dating. Earth Planet. Sci. Lett. 179, 91–99.
Staiger, J.W., Marchant, D.R., Schäfer, J.M., Oberholzer, P., Johnson, J.V., Lewis, A.R., Swanger, K.M., 2006. Plio-Pleistocene history of Ferrar Glacier, Antarctica: implications for climate and ice sheet stability. Earth Planet. Sci. Lett. 243, 489–503.
Sugden, D.E., Marchant, D.R., Potter, N.J., Souchez, R.A., Denton, G.H., Swisher, C.C.I., Tison, J.L., 1995. Preservation of Miocene glacier ice in East Antarctica. Nature 376, 412–414.
Swanger, K.M., Marchant, D.R., Schaefer, J.M., Winckler, G., Head III, J.W., 2011. Elevated East Antarctic outlet glaciers during warmer-than-present climates in southern Victoria Land. Glob. Planet. Change 79, 61–72.
Warren, K., Eppes, M.-C., Swami, S., Garbini, J., Putkonen, J., 2013. Automated field detection of rock fracturing, microclimate, and diurnal rock temperature and strain fields. Geosci. Instrum. Methods Data Syst. 2, 275–288.
Washburn, A.L., 1979. Geocryology: A Survey of Periglacial Processes and Environments. Edward Arnold, London, (406 pp.).